Growth Processes in Si/Si(111) Epitaxy Observed by Scanning Tunneling Microscopy during Epitaxy

Bert Voigtländer and Thomas Weber
Forschungszentrum Jülich, Institut für Grenzflächenforschung und Vakuumphysik, 52425 Jülich, Germany
(Received 23 May 1996)

We have studied Si/Si(111) epitaxy during the growth process at high temperatures (500–900 K) with the scanning tunneling microscope. During the growth of two-dimensional islands, we observe three different growth processes: initial sharpening of the corners of triangular Si(111) islands, nucleation in the second layer at domain boundaries of the (7×7) reconstruction, and growth at the island edges occurring along rows of the width of the (7×7) unit cell. During the coalescence of islands, we observe the development of a new $[11\bar{2}]$ facet growing with high growth speed. A model of hindered nucleation on the faulted part of the (7×7) reconstruction explains the experimental results. [S0031-9007(96)01458-5]

PACS numbers: 81.15.Hi, 07.79.Cz, 68.55.Jk, 68.65.+g

The characterization of the growth morphology of semiconductors is performed by either diffraction methods or real-space imaging methods. These two approaches are quite complementary. The diffraction methods [mainly reflection high energy electron diffraction (RHEED) [1]] have the advantage that they can be used during growth. On the other hand, the information on the surface morphology is quite indirect using diffraction methods. Real-space imaging methods [namely, transmission electron microscopy (TEM) [2]] have the ability to measure the morphology of the grown film directly. However, these methods are usually performed "post mortem," i.e., the growth is terminated, the sample is cooled to room temperature and removed from the growth chamber.

In the above mentioned standard analysis techniques it is only possible to achieve either the high real-space resolution or to perform dynamical measurements. Ideally, a combination of both is desirable. Recently, an effort was made to extend the capabilities of these analysis tools for semiconductor growth towards the combination of high spatial resolution and the ability to perform dynamical measurements. There are efforts to improve the spatial resolution of the RHEED technique [3] and to combine molecular-beam epitaxy (MBE) with the TEM technique [4]. In addition, new methods such as low energy electron microscopy (LEEM) [5] and reflection electron microscopy (REM) [6] have been developed which permit high spatial resolution during growth.

In addition to these semiconductor growth characterization methods, scanning tunneling microscopy (STM) has become a powerful method for the study of epitaxial growth even at the atomic level. However, in the past, STM has been limited to "snapshots" of certain growth stages. The growth was interrupted at a specific coverage, and the sample was quenched to room temperature and then transferred to the STM for imaging. There are several disadvantages of using this mode of STM operation. (i) It is not clear how the surface morphology changes during quenching. (ii) Only one coverage can be analyzed for every MBE grown sample; STM is a time-consuming method. (iii) Individual growth structures, which are, in principle, accessible by a real-space microscopy, cannot be studied in their evolution as a function of coverage. Recently, some effort was made to overcome these disadvantages [7–10].

Our approach has been to combine the ability of the STM to image the (3D) surface morphology at high spatial resolution with the ability to perform dynamical studies during growth at high temperatures. In this molecular beam scanning tunneling microscopy mode (MBSTM), we continuously image the surface during growth and have access to the evolution of the growing film. Also, the influence of local growth features, such as defects on the growth, can be studied with atomic resolution.

In this Letter we report on the observation of different growth processes during Si/Si(111) epitaxy. We observed initial sharpening of island corners, nucleation of second layer growth at (7×7) domain boundaries, and the lateral growth of the islands in stripes of the width of the (7×7) unit cell along the island edges. During coalescence of islands, the growth speed of different facets could be measured. The unique feature of this method, i.e., observing the growth history of a single feature on the surface, can be used to observe the different growth processes occurring in Si/Si(111) epitaxy better than with the regular STM mode. We compare our observations with the theoretical model of Shimada and Tochihara [11] for the growth of Si on Si(111).

We used a beetle type STM [9]. All piezos are surrounded by a shield for high temperature operation and to prevent deposition onto the piezos. The thermal drift is considerable when the sample temperature is raised. After one hour at a fixed temperature (600–900 K), the thermal drift decreases to ~10–20 Å/min. The Si evaporator is located under an angle of 50° from the sample normal. Because of the open design of the STM, the molecular beam can be directed towards the sample, which is located

0031-9007/96/77(18)/3861(4)$10.00 © 1996 The American Physical Society

in the STM position. Evaporation is done continuously while the STM is scanning the growing film. Part of the MBE beam impinging on the sample is shaded by the tip, which reduces the growth rate in the scanned area [9].

The MBSTM measurements were performed in an ultrahigh vacuum chamber (base pressure $= 3 \times 10^{-11}$ mbar). Si was evaporated from a homemade electron beam evaporator. The sample was cleaned by a 30 s anneal to 1500 K at a pressure below $=5 \times 10^{-10}$ mbar. Because of the crystallography of the Si(111) surface, the growth in the vertical direction occurs in units which are 3.1 Å high. We call this unit of 1.56×10^{15} atoms/cm^2 one monolayer.

The homoepitaxial growth of Si on Si(111) is a well studied growth system. In particular, a recent STM study showed details on the nucleation and the subsequent growth of Si on Si(111) by imaging snapshots at different growth stages [12]. However, the dynamics of growth processes can only be observed by repeated imaging of the same area during growth.

Figure 1(a) shows a triangular Si(111) island (outward normal of the island edges along $[\bar{1}\bar{1}2]$ directions) on the Si(111) substrate. The substrate is out of contrast and not shown. A (7×7) reconstruction is observed on the island. When we superimpose grids through the corner holes of the (7×7) reconstruction, two mutually shifted grids are necessary for the right and left part of the island. In the lower right of the island a more disordered region exists. Between the two (7×7) domains indicated by the grids, a domain boundary occurs. In Fig. 1(b), at a later stage during growth ($T = 670$ K), the nucleation of the growth in the next layer is observed just at this domain boundary [white area in Fig. 1(b)]. A preferred nucleation at domain boundaries on the bare Si(111) substrate has been previously observed [12]. However, on the epitaxial islands, this nucleation behavior at surface defects has not been observed, and only the ability to image the surface before and after the nucleation at the same location gives direct access to this nucleation event on the islands.

Another characteristic process during growth is the sharpening of the island corners during growth. Figure 1(a) shows the image of a pregrown island (evaporator off while imaging at $T = 670$ K). In this image the island corners are quite round. The image displayed in Fig. 1(b) was scanned during growth. In this case, the island corners become sharp. When the evaporation is stopped, the adatom concentration in the 2D lattice gas on the Si substrate decreases, and, due to this lower "adatom pressure" around the islands, atoms detach from the islands, leading to rounder island corners. Atoms are most easily evaporated from the island corners because of the reduced coordination compared to the compact island edges.

One important growth process is the lateral growth of the islands. Does the growth occur atom-by-atom along the island edges, or are the stable building units larger?

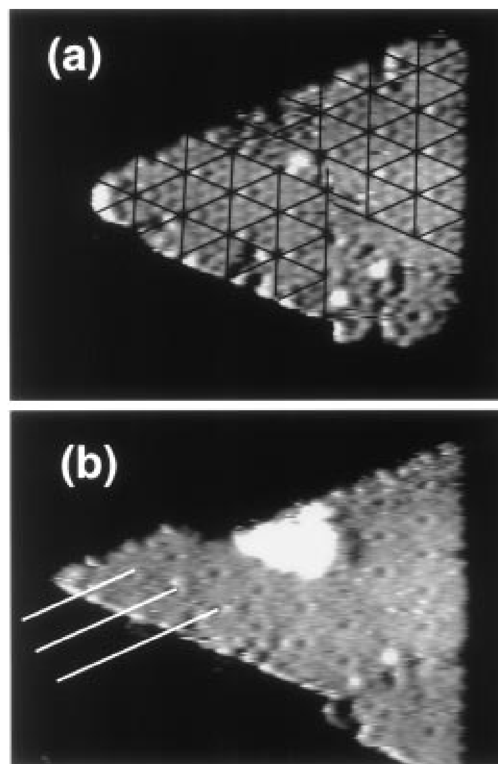

FIG. 1. STM image of a Si(111) island during growth at 670 K. Comparing (a) and (b), different growth processes can be identified: growth in stripes of the width of the (7×7) unit cell along the island edges, nucleation of next layer growth at (7×7) domain boundaries, and sharpening of the island corners during growth.

When we compare Figs. 1(a) and 1(b), a stripe of silicon of the width of the (7×7) unit cell has grown in the left of Fig. 1(b). The distance between the corner holes on the island, indicated by white lines, shows that the width of the grown stripe is, indeed, the width of one (7×7) unit cell, i.e., 26.9 Å.

While the identification of certain growth processes is already possible from the two images shown in Fig. 1, the continuous observation of growth as a function of time gives even more information, for instance, on the energy barriers related to these processes. In Figs. 2(a)–2(f) so-called "difference images" are shown. In the difference image, a reference image is subtracted from each image. In this scheme the new material, grown subsequent to the reference image, appears as white. In Fig. 2(a) we see that the first growth process occurring is the sharpening of island corners [arrows in Fig. 2(a)]. The next process is the nucleation on top of the one monolayer high Si islands at the domain boundaries [Fig. 2(b)]. Since we often find more material in the second layer than the amount which was deposited in this layer (assuming isotrope deposition), this shows that an upward mass transport must occur during growth. Only subsequent to this stage is lateral growth observed. White stripes of the width of the (7×7) unit cell run along the island edge from the

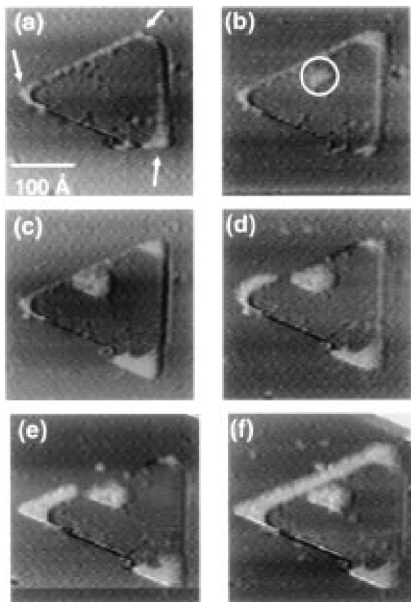

FIG. 2. Difference images showing the course of the growth processes during Si/Si(111) epitaxy ($T = 670$ K). In the difference images new material grown subsequent to a reference time is highlighted in white. Images (a)–(f) were recorded 90, 508, 1298, 2108, 3003, and 4074 s after the reference image was taken.

left corner to the upper right corner of the triangular island in Figs. 2(d)–2(f).

This sequence, sharpening of island corners, growth in the second layer, and finally lateral growth, provides information on the relevant energy barriers for the different growth processes. The attachment of material to the island corners is the first process occurring during the growth, and therefore the corresponding energy barrier is the lowest. The nucleation of a new row along the island edge, occurring as the last process, is associated with the highest energy barrier. The nucleation on top of the island occurs long before coalescence of islands. The amount of Si nucleated on top of the islands is much larger than expected from isotropic deposition. This shows that the process of upward hop on top of the 2D islands and nucleation at the domain boundaries has a lower energy barrier than the nucleation of the lateral growth at the step edge. This gives rise to the initial multilayer growth observed in Si/Si(111) epitaxy [12].

Now we turn to effects occurring during the coalescence of two islands. In the case of the growth of a 2D crystal (island), the step edge is the growth facet. The term $[hkl]$ facet refers to the step edge with the outward normal along the $[hkl]$ direction on the surface. On the Si(111) surface, two different low index step edge facets exist: steps along $[\bar{1}\bar{1}2]$ and steps along $[11\bar{2}]$ directions. These two different facets may grow with different growth speeds. It is a general law of crystal growth that only those facets which advance slowest during growth survive during the growth process [13]. Therefore, during the growth of single islands, we observe the formation of two-dimensional triangular islands with facets along $[\bar{1}\bar{1}2]$ directions (slow growing facets). In Fig. 3 we show that after the coalescence of two triangular islands a new, fast growing facet along $[11\bar{2}]$ direction occurs. In Fig. 3(a), two triangular islands with step edges along $[\bar{1}\bar{1}2]$ directions, which almost touch, are shown. In this case, the islands are two monolayers (6.4 Å) high, and the first and second layer grow almost simultaneously. Upon coalescence of the islands, fast growth along the $[11\bar{2}]$ facet on the right [arrows in Figs. 3(b) and 3(c)], and then on the left [arrows in Figs. 3(d)–3(f)], of the coalescence region occurs.

Annealing experiments show that the equilibrium form of the Si islands on Si(111) is hexagonal [9]. This indicates that the different observed growth speeds are related to the growth kinetics. In the following, we show how important the influence of the surface reconstruction is to understand the growth kinetics of Si(111) islands. The Si(111) substrate is itself reconstructed. The unit cell of the (7×7) reconstruction consists of two triangles, one without a stacking fault (U), and one with a stacking fault (F) (in the upper monolayer) relative to the substrate structure. During growth, this (7×7) reconstruction of the substrate has to be lifted, and the atoms have to arrange into the bulk structure. This reordering process is very different for the U and F half units of the

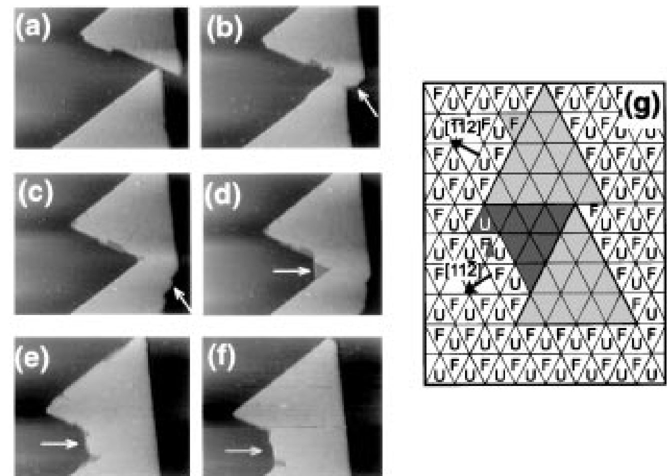

FIG. 3. STM images showing the coalescence of two islands. After coalescence, preferred growth along $[11\bar{2}]$ facets is observed. The image size is 1400 Å × 1100 Å, and the growth temperature is 700 K. In (g) the principle arrangement of the U and F parts of the (7×7) unit cells on the substrate around two coalescing islands is shown. The higher growth speed along the $[11\bar{2}]$ direction can be explained by a high energy barrier for the initial nucleation of the growth on a faulted triangle (F) in the case of the slow growing $[\bar{1}\bar{1}2]$ facet, and a low barrier for the nucleation at an unfaulted triangle (U) for growth at the fast growing $[11\bar{2}]$ facet. Images (b)–(f) were recorded 396, 1056, 1320, 1848, and 2376 s after the image shown in (a). The complete growth sequence is available as a movie on the World Wide Web [14].

(7×7) reconstruction. While the unfaulted part of the reconstruction can be easily overgrown, this is not so for the faulted part because the stacking fault has to be removed during overgrowth, which costs additional energy. Shimada and Tochihara derived a model of the Si/Si(111) growth from the following postulates [11]: (i) The building blocks of the lateral growth are the F and U subunits of the (7×7) unit cell, (ii) the destruction of the faulted triangles of the substrate reconstruction is the rate limiting step for the lateral growth at Si islands, and (iii) the overgrowth of the unfaulted halves at the step edges is rapid. Postulate (i) of this model is in accord with our experimental findings, that the lateral growth of the Si(111) islands occurs in stripes of the width of the (7×7) unit cell along the slow growing step edges, and that the island edges of the Si islands are in registry with the substrate (i.e., island edges run along the corner holes of the substrate reconstruction).

In the following, we show how the observed higher growth speed along $[11\bar{2}]$ facets can be explained in the framework of the model of Shimada and Tochihara [11]. In Fig. 3(g) we see that the growth in the $[\bar{1}\bar{1}2]$ direction has to start by nucleating on a faulted triangle because only this has a common edge with the $[\bar{1}\bar{1}2]$ step. According to postulate (ii), this nucleation event is energetically costly and therefore slow. On the other hand, nucleation of growth at the fast growing $[11\bar{2}]$ facet starts with overgrowth on an unfaulted triangle [an easy process according to postulate (iii)]. When the nucleation on an unfaulted triangle occurred, the existence of a "macro kink" [indicated by an arrowhead in Fig. 3(g)] facilitates further overgrowth of a faulted triangle. Adatoms can get trapped at this kink and facilitate overgrowth of this unit. This shows that the growth along the $[11\bar{2}]$ facet occurs faster than the lateral growth at the $[\bar{1}\bar{1}2]$ facet.

Also other experimental observations can be explained straightforwardly by the model. From the analysis of movies, which we take continuously during growth, we find that it takes some time before a new row nucleates at the slow growing facet. However, once a new row has nucleated at the island edge, further growth of the stripe is fast. This shows that, indeed, according to postulate (ii), the rate determining step during lateral growth is the nucleation of a new stripe on a F triangle of the unit cell. Because of the existence of a macro kink, neighboring U and F units can be overgrown in quick succession, leading to the fast growth of a stripe of the width of the (7×7) unit cell. A further observation during coalescence of islands (Fig. 3) is that the slow growing facets are straight, while the fast growing facets have a rougher appearance. Also, this observation can be explained in the framework of the model of Shimada and Tochihara [11]. Fluctuations during growth of the fast growing facet give rise to the formation of small facets of the slow growing (more stable) facet and hence to rougher step edges.

When we analyze the material distribution during growth, we find that about one-half of the growing material grows at the fast growing facets and the other half grows at all the other slow growing facets. This shows that material transport along island edges and around the corners is rapid enough to supply the material to the fast growing facets.

In summary, during growth of a pre-existing 2D Si island on Si(111), the following growth processes are observed by the use of the MBSTM method. Initial sharpening of the island corners occurs first, and is therefore associated with the lowest energy barrier. This is consistent with the fact that the sharpening of the island edges involves growth on an unfaulted triangle of the (7×7) unit cell [Fig. 3(g)]. Before lateral growth starts, nucleation on top of the island occurs. The largest energy barrier is associated with this latest occurring growth process: the rearrangement of the atoms in a faulted triangle of the reconstruction to a bulk structure during overgrowth. This is the rate limiting process for the lateral growth of the island along a stripe of the width of the (7×7) unit cell. The easier overgrowth of unfaulted triangles gives rise to the observed fast growth speed along the $[11\bar{2}]$ facet during the coalescence of islands.

[1] J.H. Neave, B.A. Joyce, P.J. Dobson, and N. Norton, Appl. Phys. A **31**, 1 (1983).

[2] D.J. Eaglesham, E.P. Kvam, D.M. Mahler, C.J. Humphreys, and J. Bean, Philos. Mag. **59**, 1059 (1989).

[3] M. Ichikawa, Mater. Sci. Rep. **4**, 147 (1989).

[4] F.K. LeGoues, M.C. Reuter, J. Tersoff, and M. Hammar, Phys. Rev. Lett. **73**, 300 (1994).

[5] E. Bauer, M. Mundschau, W. Swiech, and W. Telips, Vacuum **41**, 5 (1990).

[6] K. Takayanagi, K. Yagi, K. Kobayashi, and G. Honjo, J. Phys. E **11**, 441 (1978).

[7] T. Hasegawa, M. Kohno, S. Hosaka, and S. Hosoki, Phys. Rev. B **48**, 1943 (1993).

[8] U. Köhler, L. Andersohn, and B. Dahlheimer, Appl. Phys. A **57**, 491 (1993); B. Voigtländer and Th. Weber (to be published).

[9] B. Voigtländer and A. Zinner, Appl. Phys. Lett. **63**, 3055 (1993); B. Voigtländer, A. Zinner, and Th. Weber, Rev. Sci. Instrum. **67**, 2568 (1996).

[10] C. Pearson, M. Krueger, and E. Ganz, Phys. Rev. Lett. **76**, 2306 (1996).

[11] W. Shimada and H. Tochihara, Surf. Sci. **311**, 107 (1994).

[12] U. Köhler, J.E. Demuth, and R.J. Hamers, J. Vac. Sci. Technol. A **7**, 2860 (1989).

[13] K. Spangenberg, *Handbuch der Naturwissenschaften, Bd. 10* (Gustav Fischer Verlag, Jena, 1934); Th. Michely, M. Hohage, M. Bott, and G. Comsa, Phys. Rev. Lett. **70**, 3943 (1993).

[14] http://www.kfa-juelich.de/video/voigtlaender